MATEC Web of Conferences **367**, 00016 (2022) https://doi.org/10.1051/matecconf/202236700016
Power System Engineering 2022

ORC and sCO_2 cycle for high temperature WHR applications

Tereza Kubíková[1*]

[1]Department of Power System Engineering, Faculty of Mechanical Engineering, University of West Bohemia in Pilsen, Univerzitni 22, 306 14, Pilsen, Czech Republic.

Abstract. This article suggests a suitable closed thermodynamic cycle for waste heat from a cement plant by using alternative working fluids. A pair of closed working cycles is compared: supercritical CO_2 cycle (sCO_2) and the Organic Rankine Cycle (ORC). In the case of ORC, it was necessary to choose a suitable working fluid. The goal is to minimize the ODP (Ozone Depletion Potential) and GWP (Global Warming Potential), to maximize the thermal efficiency and to optimize the minimum working temperature difference (pinch points, approach points), the temperature profiles of the heat exchangers and their working pressure and temperature, which affects the cost. Both cycles (ORC and sCO_2) including a detailed component analysis are calculated using Python in Spyder IDE, which includes all the libraries for this task. According to the results of the calculations, the ORC cycle was chosen for further calculations of the components (condenser and turbine). The most suitable working fluids with high efficiency are hexamethyldisiloxane (MM), ethylbenzene and toluene, from which toluene was selected.

1 Introduction

The advantage of a closed cycle in comparison to an open cycle (e.g. the Ericsson-Brayton cycle of a gas turbine [1] [2]) is that it can work with a different fluid than the combustion product and ambient air. On the other hand, a closed cycle needs a heat exchanger, which transforms heat from the combustion products to the cycle working fluid. The most common example of a closed cycle is the Rankine-Clausius cycle using steam as a working fluid; it is used mainly in regular power plants. However, the thermodynamic properties of steam are not ideal for all applications. The waste heat recovery (WHR) typically has to deal with relatively low temperature, which implies lower thermal efficiency even in an ideal Carnot cycle (which uses the hard to achieve isothermal heat exchange). Some examples of thermal cycles and their working temperature gradients and heat powers are plotted in Fig. 1 (from Liu [3])

* Corresponding author: tereza.kubikova@doosan.com

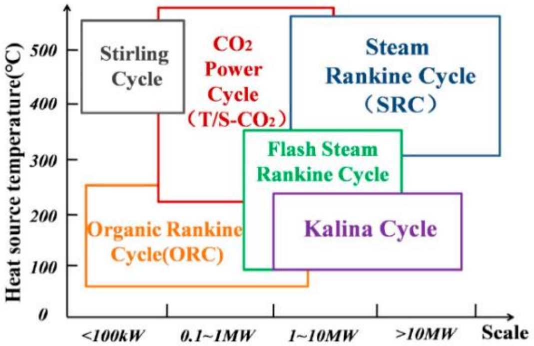

Fig. 1 Diagram of closed thermal cycles - comparison of their powers and temperatures.

1.1 WHR usage

Waste heat is lost into the atmosphere or a condenser if not recovered. It can be recovered by adding a new cycle, e.g. ORC, sCO2, CCGT (Closed Cycle Gas Turbine), Kalina cycle etc. and the heat can be used for electric power generation or for heating. The heat can be recuperated locally, i.e. the hot combustion products at the turbine outlets are used to pre-heat the working fluid before the heater inlet. Thus the amount of energy needed is decreased. In the case of an alternative cycle (e.g. due to better thermodynamic properties of an alternative working fluid for the low-potential heat), the combustion product (source) transfers the thermal energy to the working fluid of the external cycle in a heat exchanger [3], which increases the total power output and reduces the specific emissions.
Fig. 2 shows the classification of WHR sources according to Liu [3]. Alternative classification (Table 1) is suggested by Johnson [4] in his study according to the heat quality, i.e. the usable temperature gradient, but Jouraha [5] suggests slightly lower temperature values:

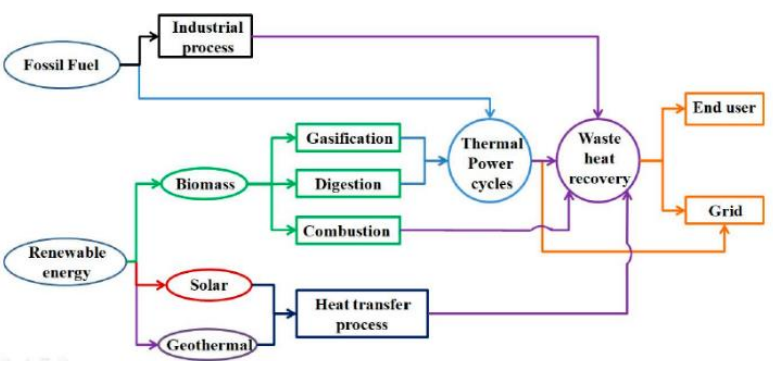

Fig. 2 WHR source classification. Figure from Liu [3]

Table 1. Temperature Classification of WHR sources.

High (>650 °C) or by [4] (>400°C)	Nickel refining furnace Steel electric arc furnace Glass melting furnace Coke oven Iron cupola Copper refining furnace
Medium (230-650°C) or by [4] (100-400°C)	Steam boiler exhaust Gas turbine exhaust Cement kiln Heat treating furnace Reciprocating engine exhaust
Low (<230°C) or by [4] (<100°C)	Cooling water from: Furnace doors Air compressors Internal combustion engine

Low temperature applications need different materials and types of heat exchangers. The reason is that corrosion can form at lower temperatures. The methods of WHR include the transfer of the waste heat into the cycle as a new external heat source. Again, a higher quality of heat produces a higher thermal efficiency of the entire cycle.
The heat recuperation consists mainly of several types of heat exchangers [5]:

- *Regenerators for air* (rotational, recuperative) – they use the waste heat of combustion products of low and middle potential sources (turbine outputs, recovery of furnaces or compression boilers)
- *Recuperation or economization* – heat exchangers with tubes or fins, which recover the middle and low potential heat for preheating of incoming fluid (e.g. water)
- *Waste heat boilers* – recovery of high potential heat to produce steam
- *Heat tubes* – heat pump which transfers the heat along a tube by using evaporation and condensation of working fluid (water, acetone, methanol, ammonia)
- *HRSG* – Heat Recovery Steam Generator – system of the previously mentioned exchangers for heating up, boiling and overheating a different working fluid (steam). Such a device is used in gas-steam turbines, where it uses the heat from the output of a BC turbine to the Rankin steam cycle
- *Device for direct transformation of heat to electricity* – thermocouples or thermophotovoltaic cells (not yet in mass use due to their low efficiency)

1.2 Organic Rankine Cycle (ORC)

The Organic Rankine cycle (ORC) is a closed cycle similar to the Rankine cycle with steam, but it uses an organic compound as a working fluid. ORC is suitable for middle and low potential waste heat sources, which are not suitable for the steam cycle, and for renewable energy sources such as solar, geothermal or biomass. [7]
Fig. 3 shows the T-s diagram and scheme of ORC cycle according to Colonna [7]. The following processes can be seen in the T-s diagram:

- **1-2** Pump – isentropic pressurizing of liquid fluid to higher temperature and pressure
- **2-3** Cold side of Recuperator – heat intake from expanded working fluid in process 5-6, it preheats the working fluid before the main heat input
- **3-4** Heat exchanger – isobaric heat input from primary WHR source, heating up, boiling and eventually overheating of the working fluid
- **4-5** Isentropic (according to Fig. 3 polytropic) expansion in turbine (or expander) to get mechanical energy. At the stage 5, the working fluid is typically hot enough to use the recuperation effectively
- **5-6** Hot side of recovery heat exchanger – the expanded fluid gives the heat to compressed fluid 2-3. Without this part, the heat would be lost in the condenser
- **6-1** Condenser (water, air) – isobaric-isothermal heat sink

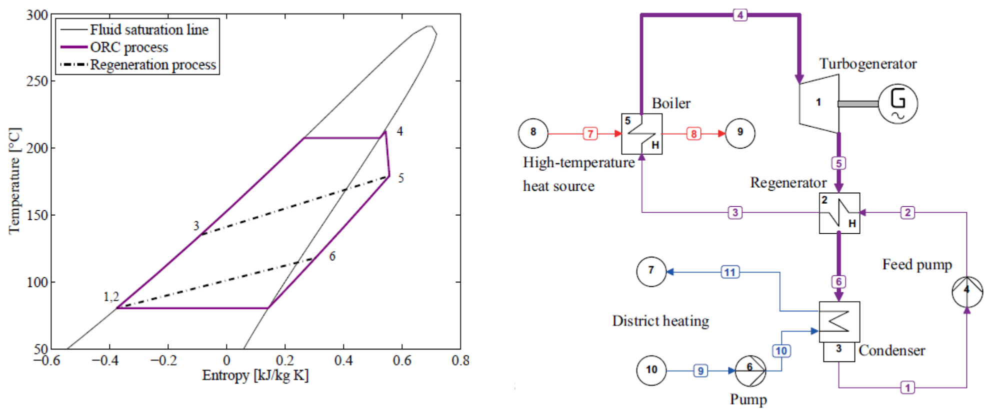

Fig. 3. (left) T-s diagram of ORC cycle; (right) scheme of ORC cycle. Both figures from the work of Colonna [7]

The organic fluid may lose stability or ignite due to high temperatures. To avoid this, a secondary heat transfer loop is added between the primary source and the boiler. This loop transfers the heat into the ORC cycle. A thermal oil is used as the transfer fluid; according to CoolProp tables [8], this oil is stable up to 400°C [7].

1.3 Supercritical CO_2 cycle (sCO_2)

The supercritical CO_2 cycle is a closed cycle similar to the Brayton or Rankine cycle, the working fluid is carbon dioxide (CO_2) and both heat input and output take place at supercritical conditions (in contrast to ORC, where the pressures, relative to the working fluid, are similar to conventional cycles). The critical temperature of CO_2 is 30.98 °C and the critical pressure is 73.8 bar. Thus this working fluid is suitable for low-potential heat sources. Fig. 4 shows the T-s diagram two variants of the CO_2 cycle: the supercritical Brayton cycle with all points above the critical one (red line in Fig. 4) and the classical Rankine cycle using phase transitions (blue line in Fig. 4). The maximum usable pressure is limited by the mechanical stability and it is usually 200 – 300 bar. Therefore the pressure ratios are expected to be low, $\pi \approx 2 - 3$, maximum $\pi \leq 4$. There is no phase transition during the cycle. The main advantage is the saving of compression work due to advantageous density dependence on the pressure near the critical point [9] [10] [11]. Fig. 5 shows the scheme and the cycle diagram according to Machionni [10].

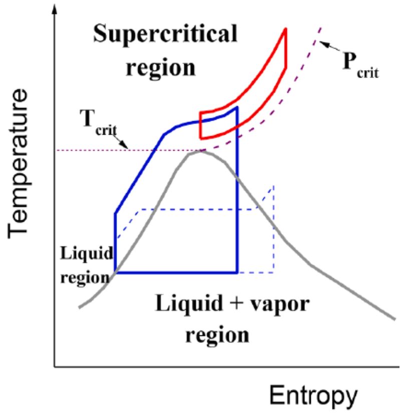

Fig. 4. Figure 4 T-s diagram of CO_2 supercritical Brayton (red) cycle and of classical CO_2 Rankine (blue) cycle. (from Wu [11])

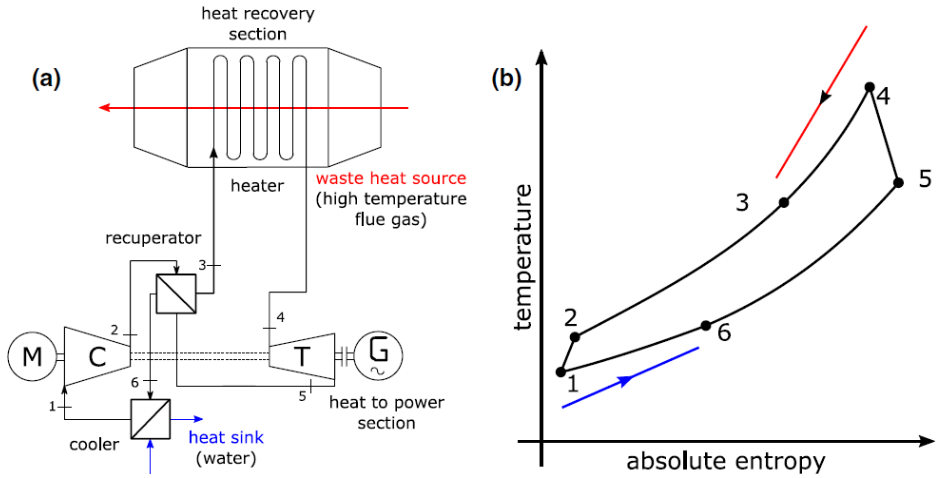

Fig. 5. (left) scheme of the supercritical CO_2 cycle, (right) T-s diagram of sCO_2 cycle with recuperation. (from Marchioni [10])

- **1–2** Compression
- **2–3** Cold side of Recuperator
- **3–4** Heat intake from primary source (WHR)
- **4–5** Expansion in a turbine or expander
- **5–6** Hot side of Recuperator – heat transfer to the colder compressed fluid (**2–3**)
- **6–1** Cooler – Heat sink from the cycle. The goal is to approach the critical point in order to save the compression work (the main advantage against the classical Brayton cycle).

https://doi.org/10.1051/matecconf/202236700016

2 Comparison and evaluation of both cycles

The main aim of this article is to compare the applicability of the sCO_2 and ORC cycles for the recovery of waste heat from a cement plant with the parameters listed in Table 2.

Table 2. Cement plant parameters considered for this study

Waste heat power (combustion products)	15 MW_t
Inlet temperature at primary exchanger	380 °C
Outlet temperature at primary exchanger	180 °C
Cooling air (atmosphere)	Temperature ~ 20 °C, humidity ~ 15 %
Power net frequency	50 Hz

2.1 Supercritical sCO_2 cycle

Fig. 6 shows the T-s diagram of a supercritical CO_2 cycle with recuperation by using the specific parameters for this study. Temperatures and pressures of the main points are listed in Table 3.
The red dashed line in Fig. 6 represents the process in the primary heat exchanger, which is heated by using the combustion products from the cement plant with a thermal power of 15 MW. The combustion products cool from 380 °C down to 180 °C. The approach point (the temperature difference between the cold and hot sides of the primary heat exchanger at the turbine inlet) is 20 °C; the pinch point (ΔT at exchanger inlet) is 8 °C. The blue dashed line represents the primary heat sink which is an air heat exchanger with an intake air temperature of 20 °C and outlet temperature difference of 10 °C (thus the outlet air temperature is 30 °C).

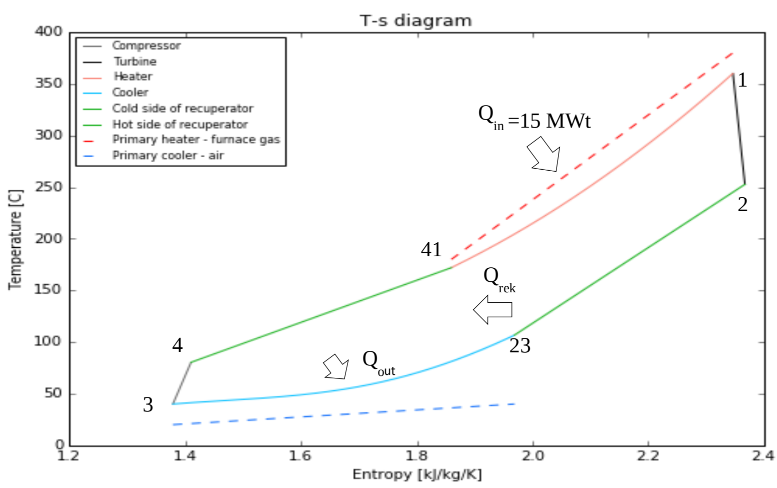

Fig. 6. T-s diagram of sCO_2 cycle with recuperation (green lines).

Fig. 7, Fig. 8 and Fig. 9 show the processes inside the exchangers: primary exchanger between combustion products and working fluid before turbine inlet (Fig. 7), recuperation exchanger between expanded and compressed working fluid (Fig. 8) and the heat sink to the ambient air (Fig. 9). The primary heat exchanger (Fig. 7) cools the combustion products from 380 °C down to 180 °C with a total heat power of 15 MWt to study the parameters (Table 2).

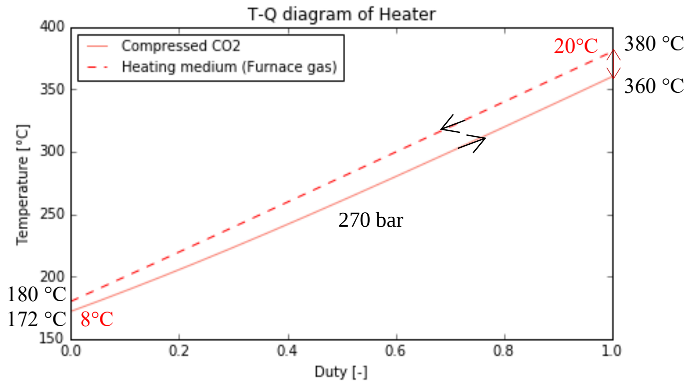

Fig. 7. T-Q diagram of primary and secondary heat input loop of the sCO_2 cycle.

Fig. 8 shows the T-Q diagram of the cold and hot side of the recuperator. The pressure on the hot side is 96.4 bar (i.e. supercritical). It is cooled from 252.6 °C down to 106.7 °C. The working fluid on the cold side is heated from 80.3 °C up to 172 °C at a pressure of 270 bar. The total heat power of this recuperator is 10.3 MW_t. The minimum temperature difference is 26.4 °C and it occurs at the cold end of the exchanger. Therefore, it is not necessary to solve the issues connected with a possible pinch point appearing near the centre of the exchanger due to the strong heat capacity variations near the critical point [9] [19]

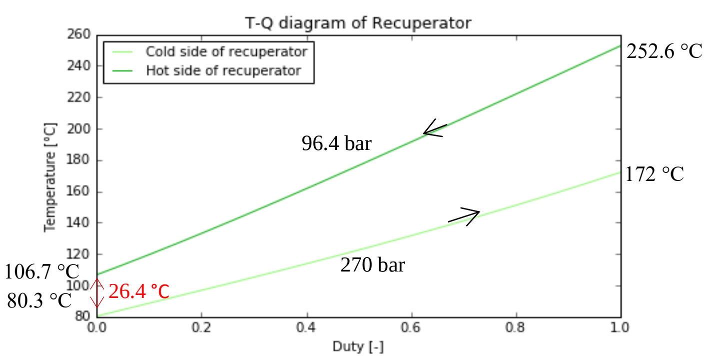

Fig. 8. T-Q diagram of sCO_2 cycle – cold/hot side of the Recuperator

Fig. 9 displays the temperature profile at the primary air heat exchanger. The supercritical CO_2 is cooled from 105.8 °C down to 40 °C (temperature close to critical). Note the temperature profile is strongly non-linear due to steep changes of heat capacity near the critical point. The pinch point appears at the cold end of the exchanger reaching a value of 20 °C. The exchanged heat power is 11.5 MWt.

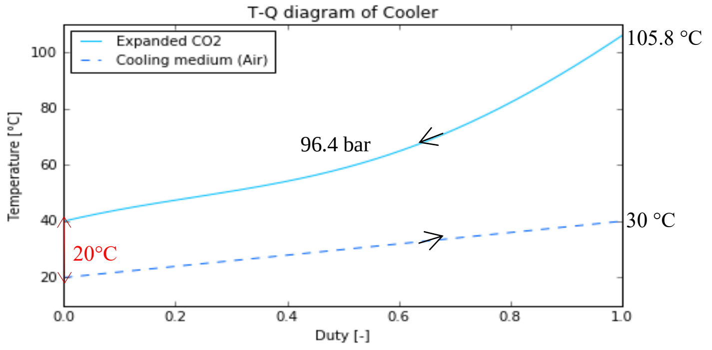

Fig. 9. T-Q diagram of sCO2 cycle – primary heat sink into the ambient air

Properties of sCO_2 during the cycle

By using CoolProp tables we are able to calculate the working fluid properties (e.g. enthalpy, entropy, density, temperature, pressure…) at any point of the cycle. Below, we publish the properties in the main points of the cycle (1 – 41).

Table 3. Selected working fluid properties at main points of the sCO_2 cycle

Point	**Volumetric flow**	**Temperature**	**Pressure**	**Specific heat**	**Thermal conductivity**	**Density**	**Dynamic viscosity**	**Kinematic viscosity**
	[m^3/s]	[°C]	[bar]	[J/kgK]	[W/m/K]	[kg/m^3]	[mPas]	[mm^2/s]
1	0.258	360	270	1267	0.052	225.2	0.034	0.15
2	0.571	252.6	96.4	1150	0.039	101.9	0.026	0.26
23	0.338	106.7	96.4	1428	0.031	172.3	0.022	0.13
3	0.097	40	96.4	6989	0.074	596.7	0.045	0.07
4	0.082	80.3	270	2165	0.078	710.9	0.059	0.08
41	0.146	172	270	1625	0.051	398.8	0.035	0.09

Table 3 shows these properties along the cycle. The maximum deviations can be observed near the critical point (i.e. between the heat sink and compressor) [9] [10].Table 4 shows the integral characteristics, i.e. power and efficiencies of the entire cycle. The total generated power is 3.5 MWe and the thermal efficiency calculated by both alternative formulae (1) and (2) is 23.5 % without the losses inside the cycle. Without the recuperation, the efficiency would be below 20 %.

Note, that it is not discussed here the details of flow within the system. The flow near the corners in heat exchangers produces secondary flow [13], [6], which increases the losses on the one hand and on the other, it increases the heat transfer by producing larger-scale structures travelling through the flow [14]. Such a complicated analysis would also depend on the exact design of the components, because even small geometry modifications can have an effect on the turbulent flow [15], which can switch the flow into different turbulent states [16].

The reason for the relatively low thermal efficiency of the studied cycle is the low temperature of the input thermal power combined with the relatively high temperature of the heat sink (180 °C). If it were possible to cool to a lower temperature than the suggested one, the cycle efficiency would be better.

The total efficiency can be computed by using two independent formulae (1), (2), which may produce the same result:

$$\eta(1) = (\dot{Q} - Q_{\text{rem}})/\dot{Q} \qquad [-] \qquad (1)$$

$$\eta(2) = P_{\text{net}}/\dot{Q} \qquad [-] \qquad (2)$$

$\dot{Q} = 15$ MWt is thermal output supplied to the cycle from the flue gas from the cement plant, Q_{rem} is the heat sink calculated as a difference between enthalpies (h_2 enthalpy behind the turbine, h_3 enthalpy in the condenser, h_{23} enthalpy on the hot side of the recuperator) multiplied by the mass flow according to (4). P_{net} is the plant net power output according to (5) without considering losses. In this equation is h_1 enthalpy at the turbine inlet, h_{2id} ideal turbine outlet enthalpy and h_{4id} is enthalpy of ideal compression in the pump. The total mass flow is according to formula *(3): $\dot{m} = 58.171\ kg/s$.*

$$\dot{m} = \dot{Q}/((h_1 - h_4) - (h_{41} - h_4)) \qquad [kg/s] \qquad (3)$$

$$Q_{\text{rem}} = \left((h_2 - h_3) - (h_2 - h_{23})\right) \cdot \dot{m} \qquad [W] \qquad (4)$$

$$P_{\text{net}} = \left(\left((h_1 - h_{2id}) \cdot Turbine_{eff}\right) - \left((h_{4id} - h_3)/Compressor_{eff}\right)\right) \cdot \dot{m} \qquad [W] \qquad (5)$$

The turbine efficiency contains too many non-linear phenomena [12], therefore it has been estimated only roughly: $Turbine\_eff = 0.9$. Similarly, the compressor efficiency: $Compressor\_eff = 0.7$. The heat added by using the recuperator is calculated as (6), where h_41 is enthalpy on the cold side of the recuperator and h_4 is pump enthalpy.

$$Qrekup = (h_{41} - h_4) \cdot \dot{m} \qquad [W] \qquad (6)$$

Volumetric flow rate $\dot{m}v$ is calculated by using the total mass flow (eq. (3) and the density ρ in the investigated points of the cycle as (7):

$$\dot{m}v = \dot{m}/\rho \qquad [m^3/s] \qquad (7)$$

Table 4 Overview of the sCO_2 cycle powers and efficiency

Cycle analysis without auxiliary losses		
Power	[kW]	[MW]
Net power:	3521.91	3.5
Compressor input power:	2130.97	2.1
Turbine output power:	5652.88	5.7
Recuperator power:	10344.45	10.3
Heater power:	15000.00	15.0
Cooler power:	11478.09	11.5
Thermal efficiency	[%]	/
Cycle efficiency η(1):	23.48	/
Cycle efficiency η(2):	23.48	/

2.2 Organic Rankine Cycle (ORC)

The first step in ORC cycle sketch is to select a suitable working fluid. There is a long list of possible candidates containing hydrocarbons (alkanes, arenes), alcohols, ethers, siloxanes, and even more complicated cooling fluids, which can be used in a pure form or as a mixture. The criteria for the working fluid selection are according to Darvish [17] or Quoilin [18], [8]: Environmental sustainability, mainly the Ozone Depletion Potential (ODP) and the Global Warming Potential (GWP).

- Safety issues (carcinogenity, non-flammable, non-toxic, etc.)
- Critical point (temperature and pressure)
- Thermal stability
- High evaporation heat and vapour density
- Low viscosity
- High thermal conductivity
- Low freezing temperature
- Corrosive / anticorrosive properties
- Chemical compatibility with other materials (mainly bearings)
- Good availability and low cost

2.2.1 Working fluid selection

Table 5 gives an overview of some of the high-temperature working fluids studied for the ORC cycle. The choice has been done in order to minimize the ODP and GWP criteria. Another important issue is the back pressure, which would be an issue mainly for siloxanes (e.g. M2DM, MDM, alkanes, etc.). The best compounds with these parameters are the hydrocarbons, which have health and fire-safety issues. Therefore, very good sealing is required for the cycle and simultaneously strict operation rules, which will affect the final cost of the device. Except for the listed working fluids in the Table 5, even more fluids have been investigated, (n-octane, R365mfc, R245fa), whose critical points are not suitable for the current application.
Looking at Table 5, we find the best efficiency for hydrocarbons of **toluene**, **ethylbenzene** and siloxane **MM.** Siloxane MM (hexamethyldisiloxane) has lower efficiency, but it is safer and easier to use. The highest efficiency is achieved with toluene (similarly ethylbenzene or pure benzene). A similar effect is found when using arenes p-xylene and m-xylene respectively. Those arenes are not listed in the selection because they are not yet in commercial use and there is no experience with them. Other options are alkanes: cyclopentane, cyclohexane or n-heptane, which despite their lower critical temperatures offer efficiencies similar to hydrocarbons and are already used commercially. Ethanol is interesting as it does not need recuperation, which would lower investment costs. On the other hand, there is not yet enough experience with using ethanol as a working fluid for the ORC cycle. Siloxane MDM (octamethyltrisiloxane) displays similar efficiency to MM, only the condensation pressure is lower, which makes the construction of pumps and last stage blades more complicated than for compounds with higher condensation pressures. Under different working conditions, these siloxanes and alkanes are commonly used working fluids.[20] [21]

Table 5. Possible ORC working fluids. p1 is the pressure at the turbine inlet, p2 is at the turbine outlet (with losses), p3 is condensation pressure. "Eta without rec" signifies efficiency without recuperation, "Eta rec" is efficiency with recuperation without or with losses

Working fluids	Chem. group	Tcrit [°C]	pcrit [bar]	p1 [bar]	p2 [bar]	p3 [bar]	Eta without rec [%]	Eta rec [%]	Eta rec [%]
								without losses	w/ losses
Toluene (methylbenzene)	Arene	318.2	41.3	35.0	0.120	0.099	27.3	**31.2**	**29.68**
Ethylbenzene	Arene	344.0	36.2	14.2	0.045	0.037	-	30.0	28.62
MM	Siloxanes	245.6	19.4	15.0	0.170	0.142	-	25.6	24.25
p-Xylene (para-xylene)	Arene	342.9	35.3	19.0	0.040	0.034	27.2	31.0	29.51
m-Xylene (meta-xylene)	Arene	343.7	35.4	15.5	0.039	0.033	27.3	30.9	29.43
Benzene	Arene	289.0	49.1	44.0	0.360	0.298	-	29.9	28.41
CycloHexane	Cyklo alkanes	280.0	40.8	34.0	0.360	0.300	23.9	29.6	28.17
Ethanol (Bez rekuperace)	Alkohols	241.6	62.7	50.0	0.178	0.148	28.2	-	-
CycloPentane	Cyklo alkanes	239.0	45.7	36.0	1.059	0.879	23.3	27.5	26.13
n-heptane	Alkanes	267.0	27.4	18.0	0.185	0.153	21.1	27.6	26.26
MDM	Siloxanes	291.0	14.2	8.5	0.020	0.017	15.8	24.7	23.44

3 ORC cycle with toluene as a working fluid

The heat input and heat sink are creted by using secondary circuits with suitable working fluids. In the case of heat input, a closed loop with thermal oil (Therminol VP1) is used. This oil is heated by combustion products from a cement plant. The heat sink loop is filled with a mixture of 40 % ethylene glycol (MEG) and 60 % water. This non-freezing mixture is commonly used in power plants. The heat sink was designed with a secondary loop both for the easier calculation of the water condenser and for the reasons of costs and probably a very large area of the air exchanger in case the cooling was only air according to the specifications. The suggested cycle T-s diagram is shown in Fig. 10. Here, the process **1-2** shows expansion in turbine, **2-23** - Hot side of the recuperator, **23-3** - Condenser (23-23sat is the desuperheater – superheated steam cooler, integrated in the condenser), **3-4** - Pump, **4-41** - Cold side of the recuperator, **41-1** represents the heater, which takes heat from the secondary heating loop (red and orange dashed lines in Fig. 10). Main points (temperature and pressure) of the ORC are given in Table 5.

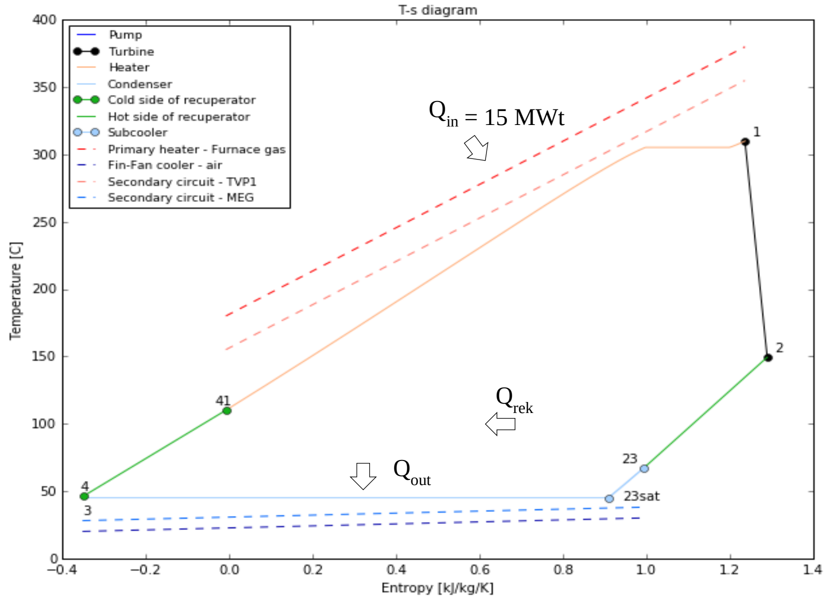

Fig. 10. T-s diagram of toluene ORC cycle with recuperation

The input temperature T_1 is calculated by using the temperature difference between the primary and secondary loop ($\Delta T = 25$ °C) and the approach point between the heated toluene and the heating loop with thermal oil ($\Delta T = 45$ °C). The turbine intake temperature is chosen in order to minimize overheating of the toluene (see Fig. 10), which increases the efficiency of the cycle. Temperature T_3 is calculated by using the temperature of the ambient air (20 °C) and the chosen TTD (Terminal Temperature Difference) of the condenser (7 °C) or the TTD between the primary and secondary cooling loop (8 °C) respectively. The temperature T_{41} is chosen in relation to the approach point and pressure p_1 and it is limited by the output temperature past the primary (and secondary) heat exchanger. This temperature directly affects the pinch points of the recuperator, primary and secondary heat exchanger as well. Pressure p_1 at the turbine inlet is chosen according to the conclusions of works [22] and [23] in order to keep away from the critical point (NRB – Near-critical Region Boundary). Condensation pressure p_3 corresponds to the condensation temperature T_3.

T-Q diagrams of ORC cycle with toluene as a working fluid

We show the T-Q diagrams similarly as in the case of sCO_2 in the previous section. These diagrams allow us to detect pinch/approach points and help to better design the heat exchangers.

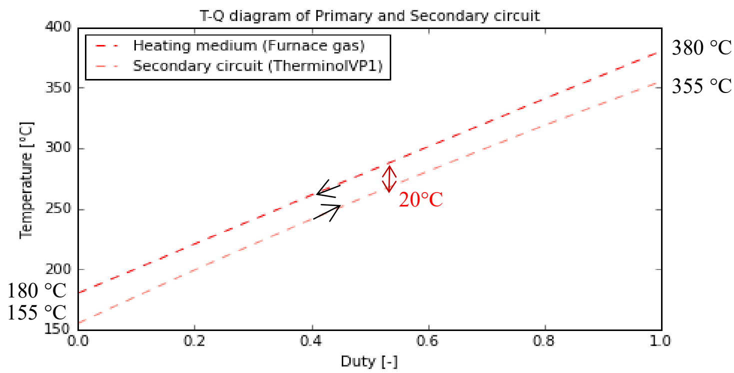

Fig. 11. T-Q diagram of primary and secondary heat input loop of the ORC cycle.

Fig. 11 shows the cooling of the combustion products from the cement furnace and heating of the thermal oil in the primary loop. The temperature difference is chosen to be 25 °C to keep the temperature gradient for heat transfer. The minimum ΔT (the pinch point) appears in the middle of the exchanger, but the heat transfer is effective enough even with this ΔT.

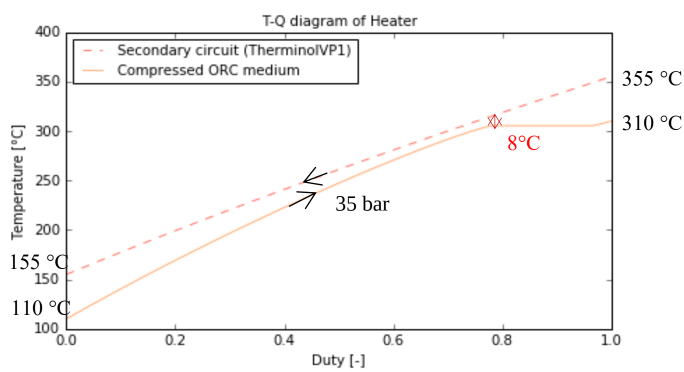

Fig. 12. T-Q diagram of secondary heating loop (Therminol VP1/toluene)

The T-Q diagram in Fig. 12 shows the heating of toluene in the secondary loop by thermal oil (dashed line). The approach point between the working fluids has been optimized to ΔT = 45 °C, thus the admission temperature T_1 is 310 °C and the pinch point has been calculated to be 8 °C. To the right of the pinch point can be observed the isothermal evaporating curve followed by very small overheating of the toluene. Generally, it is better to overheat the organic fluids less (mainly the dry types). First, overheating affects the admission temperature T_1, second, these materials may not be stable enough at higher temperatures and, third, lower overheating increases the efficiency (mainly of the dry materials).

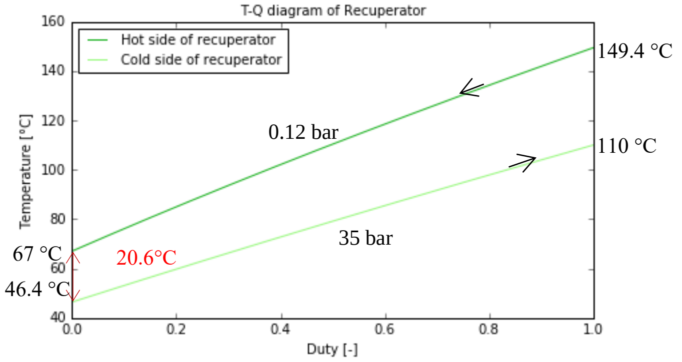

Fig. 13. T-Q diagram of recuperator

Fig. 13 shows the recuperation, which cools the expanded hot toluene and heats the compressed cool toluene before the main heater. The hot toluene cools from 149.4 °C down to 67 °C. Compressed cold toluene heats from 46.4 °C up to 110 °C. The pinch point of ΔT = 20.6 °C appears at the cold end of the exchanger.
The heat sink is formed by a condenser (isothermal light blue line in Fig. 14), the heat transfers into the MEG mixture in a secondary loop, which is cooled by air. The toluene cools from 67 °C down to 45 °C, at which it condenses, heating the MEG from 28 °C to 38 °C with a pinch point of 7 °C. The temperature difference at the primary and secondary exchanger is kept constant at 8 °C and the cooling air heats from 20 °C to 30 °C.

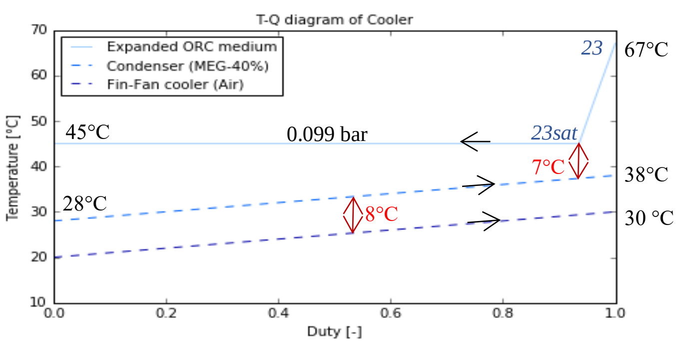

Fig. 14. T-Q diagram of ORC cycle – primary (air) and secondary (MEG) heat sink loop

The minimum temperature differences in the exchangers are summarized in Table 6 for clarity:

Table 6. Minimum temperature differences along the cycle

Minimum temperature difference [°C]	
Minimum dT of Primary heater:	19.89
Minimum dT of Secondary heater:	8.25
Minimum dT of Recuperator:	20.62
Minimum dT of Primary Cooler:	8.00
Minimum dT of Secondary Cooler:	7.66

Properties of ORC with toluene during the cycle

Table 7 summarizes the properties of the working fluid (toluene) at the main points of the cycle. The mass and volumetric flow rates are calculated similarly as for sCO_2 cycle (eq. (7)). The mass flow rate is 24.07 kg/s.

Table 7. Selected working fluid properties at the main points of the cycle

Point	Volumetric flow	Temperature	Pressure	Specific heat	Thermal conductivity	Density	Dynamic viscosity	Kinematic viscosity
	[m^3/s]	[°C]	[bar]	[J/kg/K]	[W/m/K]	[kg/m^3]	[mPas]	[mm^2/s]
1	0.180	310	35	1599	0.0517	130.6	0.0162	0.124
2	76.520	149	0.12	1297	0.022	0.315	0.0097	30.97
23	74.280	67	0.12	1213	0.014	0.324	0.0079	24.36
23sat	0.029	45	0.12	1767	0.012	0.347	0.0074	21.32
3	0.029	45	0.099	1767	0.125	843	0.4408	0.52
4	0.028	46	35	1991	0.126	845	0.4475	0.53
41	0.030	110	35	3590	0.109	784	0.2580	0.33

The properties of toluene at the displayed points is calculated according to CoolProp tables with pressure and temperature or dryness as the control parameters. The heat capacity of toluene near condensation is much lower than that of water. The thermal conductivity and viscosity of toluene reach lower values near the condensation point than water. The density at point 23sat (saturation) is 5× smaller than the density of steam, while its density at point 3 (fully condensed) is close to the density of water. From the comparison of the densities during the ORC and CO_2 cycle, it can be seen that the density of sCO_2 is several times higher, because CO_2 is single-phase and its behaviour is close to the properties of water, while the ORC medium undergoes heating and evaporation (possibly overheating). It follows from the properties of the working fluids, that exchangers and a suitable working medium must be thoroughly designed for a WHR power plant.

Thermal efficiency and power

Table 8 shows the total net power of the ORC cycle and the powers of the individual components. The pump has much smaller input power than the sCO_2 cycle. The cooler power is separated into the Steam superheat cooler power and the Steam condenser power. The thermal efficiency of the entire cycle is calculated according to formulae (1) and (2); both methods return the same value, as expected.
Table 9 shows the values of the estimated efficiencies of the components and their impact on the total power of the cycle and its components. The turbine power is estimated to decrease to 4.6 MW_e (4.8 MW_e without losses), the pump input power increases slightly when considering losses. The net power plant power decreases to 4.5 MW_e (4.7 MW_e without losses).

Table 8. The powers of ORC cycle components without losses.

Cycle anylysis without auxiliary losses		
Power	[kW]	[MW]
Plant net power output:	4680.6	4.7
Heater power:	15000.0	15.0
Turbine output power:	4804.9	4.8
Pump input power:	124.3	0.1
Recuperator power:	2873.9	2.9
Cooler power:	10319.4	10.3
Steam superheat cooler power:	665.4	0.7
Steam condenser power:	9653.9	9.7
Thermal efficiency	[%]	
Cycle efficiency (1):	31.2	/
Cycle efficiency (Basic cycle):	31.2	/

Table 9. Power and efficiency for the ORC cycle with losses

Cycle anylysis including auxiliary losses		
Turbine generator and gearbox efficiency:	0.973 [1]	97.3%
Pump electrical motor efficiency:	0.985 [1]	98.5%
Mechanical losses:	100.0 kW	0.1 MW
Power	[kWe]	[MWe]
Turbine output power at generator terminals:	4577.9	4.6
Pump power electrical consumption:	126.2	0.1
Plant net power output:	4451.7	4.5
Thermal efficiency	[%]	
Cycle efficiency (Cycle with losses):	29.68%	/

4 Conclusion

The primary aim of this work was the analysis and evaluation of two closed cycles for the energy use of waste heat from a cement plant (15 MW_t in flue gas cooled from 380 °C to 180 °C, cooling to ambient air at 20 °C): supercritical CO_2 and ORC. Based on the results of the calculations, the ORC cycle was chosen for further calculations of the components. The difficulty of the ORC cycle was selecting a suitable working medium. Calculations are performed for many working fluids (see Table 5) and are evaluated primarily according to their properties and achieved efficiency. The most suitable media with high efficiency are MM (hexamethyldisiloxane), ethylbenzene and toluene, of which toluene was chosen after critical evaluation, and whose properties across the cycle are summarized in Table 7. For the ORC cycle, calculations are performed first without losses and then including losses, e.g. mechanical and with defined efficiencies of the gearbox, generator and electric motor of the pump, see Table 9. The generated electric power of the ORC unit reaches 4.5 MWe with a cycle thermal efficiency (including included losses) of 29.68%. The individual parts will be designed in detail in the future.
The second aim of this work is to prove that the author is ready to achieve a master degree in mechanical engineering.

Acknowledgements
I thank my supervisor Ing. Jiří Kučera, Ph.D. for significant help with data analysis and discussions. I thank my former supervisor RNDr. Daniel Duda for help translating the article into English.

References

1. T. Adefarati a R. Bansal, “Energizing Renewable Energy Systems and Distribution Generation”, v Pathways to a Smarter Power System, 1. editor, Yildiz Technical University, Turkey: Academic Press (2019), https://doi.org/10.1016/C2017-0-03015-X
2. A. Razak, Industrial Gas Turbines, UK: Woodhead Publishing (2007), ISBN 978-1-84569-205-6
3. L. Liu, “Supercritical Carbon Dioxide(s-CO2) Power Cycle for Waste Heat Recovery: A Review from Thermodynamic Perspective”, Processes, vol. 8, n. 1461 (2020), https://doi.org/10.3390/pr8111461
4. I. Johnson, “Waste Heat Recovery. Technology and Opportunities in U.S. Industry”,U.S. Department of Energy (2008), https://doi.org/10.2172/1218716
5. H. Jouhara, Waste heat recovery technologies and applications, 6 editor, London: Thermal Science and Engineering Progress, pp. 268-289 (2018), https://doi.org/10.1016/j.tsep.2018.04.017
6. P. Boruta, T. Bujok, Ł. Mika a K. Sztekler, “Analysis of Designs of Heat Exchangers Used in Adsorption Chillers”, Energies, vol. 14, n. 23, p. 8038 (2021), DOI:10.3390/en14238038
7. P. Colonna, “Organic Rankine Cycle Power Systems: From the Concept to Current Technology, Applications, and an Outlook to the Future”, Journal of Engineering for Gas Turbines and Power, vol. 137, n. 10 (2015), https://doi.org/10.1115/1.4029884
8. S. Quoilin, “Techno-economic survey of Organic Rankine Cycle (ORC) systems”, Renewable and Sustainable Energy Reviews, vol. 22 (2013), https://doi.org/10.1016/j.rser.2013.01.028
9. K. Brun, Fundamentals and Applications of Supercritical Carbon Dioxide (sCO_2) Based Power Cycles, Sawston,UK: Woodhead Publishing (2017), ISBN 978-0-08-100804-1
10. M. Marchionni, “Review of supercritical carbon dioxide (sCO2) technologies for high-grade waste heat to power conversion”, SN Applied Sciences, n. 611 (2020), https://doi.org/10.1007/s42452-020-2116-6
11. P. Wu, “A review of research and development of supercritical carbon dioxide Brayton cycle technology in nuclear engineering applications”, Nuclear Engineering and Design, vol. 368, (2020), https://doi.org/10.1016/j.nucengdes.2020.110767
12. D. Duda, T. Jelínek, P. Milčák, M. Němec, V. Uruba, V. Yanovych a P. Žitek, “Experimental Investigation of the Unsteady Stator/Rotor Wake Characteristics Downstream of an Axial Air Turbine”, International Journal of Turbomachinery, Propulsion and Power, vol. 6, n. 3, p. 22 (2021), https://doi.org/10.3390/ijtpp6030022
13. D. Duda, J. Bém, V. Yanovych, P. Pavlíček a V. Uruba, “Secondary flow of second kind in a short channel observed by PIV”, European Journal of Mechanics, B/Fluids, vol. 79, pp. 444-453 (2020), https://doi.org/10.1016/j.euromechflu.2019.10.005

14. D. Duda, V. Yanovych a V. Uruba, "An experimental study of turbulent mixing in channel flow past a grid", Processes, vol. 8, n. 11, pp. 1-17 (2020), https://doi.org/10.3390/pr8111355
15. V. Yanovych, D. Duda, V. Uruba a P. Antoš, "Anisotropy of turbulent flow behind an asymmetric airfoil", SN Appl. Sci., vol. 3, p. 885 (2021), DOI:10.1007/s42452-021-04872-2
16. D. Duda, V. Yanovych, V. Tsymbalyuk a V. Uruba, "Effect of Manufacturing Inaccuracies on the Wake Past Asymmetric Airfoil by PIV", Energies, vol. 15, n. 3, p. 1227 (2022), https://doi.org/10.3390/en15031227
17. K. Darvish, "Selection of Optimum Working Fluid for Organic Rankine Cycles by Exergy and Exergy-Economic Analyses", Sustainability, vol. 7, n. 11, pp. 15362-15383 (2015), https://doi.org/10.3390/su71115362
18. S. Quoilin, Experimental Study and Modeling of a Low Temperature Rankine Cycle for Small Scale Cogeneration, Lutych: University of Liege - Aerospace and mechanical engineering (2007)
19. White, Martin T. Review of supercritical CO2 technologies and systems for power generation. Applied Thermal Engineering., vol. 185 (2021), https://doi.org/10.1016/j.applthermaleng.2020.116447
20. E. Macchi a M. Astolfi, Organic Rankine Cycle (ORC) Power Systems, 1 editor, Milano: Woodhead Publishing, p. 698 (2016), ISBN 9780081005101
21. T. Tartière, "A World Overview of the Organic Rankine Cycle Market", Energy Procedia - 4th International Seminar on ORC Power Systems, vol. 129 (2017), https://doi.org/10.1016/j.egypro.2017.09.159
22. Y. P. Wang, "Performance Analysis of Near-Critical and Subcritical Organic Rankine Cycle", Applied Mechanics and Materials, vol. 1, site 2448-453 (2013), https://doi.org/10.4028/www.scientific.net/AMM.448-453.3270
23. L. Pan, "Performance analysis in near-critical conditions of Organic Rankine Cycle", 7th Biennial International Workshop "Advances in Energy Studies", vol. 37, n. 1, (2012), https://doi.org/10.1016/j.energy.2011.11.033
24. A. M. Ahmed a A. R. Imre, "The effect of recuperator on the efficiency of ORC and TFC with very dry working fluid", MATEC Web of Conferences, vol. 345, p. 00012 (2021), https://doi.org/10.1051/matecconf/202134500012